

the high-speed after pulse measurement system for PMT^{*}

CHENG Ya-Ping^{1,2,3)} QIAN Sen^{1,2;1)} NING Zhe^{1,2} XIA Jing-Kai^{1,2,3}
 WANG Wen-Wen^{1,4} WANG Yi-Fang² CAO Jun² JIANG Xiao-Shan^{1,2}
 WANG Zheng^{1,2} LI Xiao-Nan^{1,2} QI Ming⁴ HENG Yue-Kun^{1,2}
 ZHAO Tian-Chi² LIU Shu-Lin^{1,2} LEI Xiang-Cui^{1,2} WU Zhi^{1,2}

¹ State Key Laboratory of Particle Detection and Electronics, Beijing 100049, China

² Institute of High Energy Physics, Chinese Academy of Sciences, Beijing 100049, China

³ University of Chinese Academy of Sciences, Beijing 100049, China

⁴ Nanjing University, Nanjing 210093, China

Abstract: A system employing a desktop FADC has been developed to investigate the features of 8 inches Hamamatsu PMT. The system stands out for its high-speed and informative results as a consequence of adopting fast waveform sampling technology. Recording full waveforms allows us to perform digital signal processing, pulse shape analysis, and precision timing extraction. High precision after pulse time and charge distribution characteristics are presented in this manuscript. Other photomultiplier characteristics, such as dark rate and transit time spread, can also be obtained by exploiting waveform analysis using this system.

Key words: Flash ADC, waveform analysis, after pulse, PMT

PACS: 29.30.-h, 29.40.Mc, 85.60.Ha

1 Introduction

As light sensors with outstanding characteristics such as high gain, low noise and fast response, photomultiplier tubes (PMT) gain popularity in nuclear and particle physics experiments, astronomy and medical diagnostics. Taking advantage of PMTs' individual photon detection capability, neutrino physics experiments[1, 2] employ hundreds of photomultiplier tubes to detect low intensity light, produced from large volumes of pure water, such as Super-Kamioka Neutrino Detection Experiment or Liquid scintillators, such as Daya Bay Reactor Neutrino Experiment.

Before PMTs start data taking mission, a series of tests have to be made to check whether every single PMT have reached their desired specifications, the gain, the transit time spread(TTS), the dark count or dark current and so on[3]. Time and charge information from PMTs are used to reconstruct event energy and vertex. After pulse occurs some time later after the initial photoelectron signal, and cannot be distinguished from true physical signals[4]. Thus for low background neutrino experiments that use large number of PMTs after pulse is troublesome background, and its features need fully studied and put into simulation to evaluate its impacts[5, 6]. The

mechanism of after pulse was found to be the ionization of the residual gases by the accelerated photoelectrons occurring inside the PMT[7, 8].

In order to generate at least 20 μ s time windows, the oscilloscopes were introduced even if their data taking speed was not so fast[9]. In case of big batch PMT tests, high speed becomes prominent issue for the test system. Compared with conventional oscilloscope test system, the flash ADC test system can continue without dead-time. While all oscilloscopes have dead-time between repetitive acquisition of waveforms and their dead-times can sometimes be orders of magnitude longer than acquisition time[10]. In our lab we have successfully implemented a high speed test system based on a desktop flash ADC(FADC).

2 Test Facility

The test system was based on a 1 GHz desktop FADC (CAEN DT5751)[11]. At 1.0×10^7 gain, the waveforms from the anode of the PMTs was about 10 mV amplitude. With the digitizer's 1 Vpp input dynamics and a programmable DC-offset, signals as large as 100 p.e. could be directly sampled by FADC and then read into the DAQ computer and analyzed using Root.

Received 14 March 2009

^{*} Supported by National Natural Science Foundation of China (10775181)

1) E-mail: qians@ihep.ac.cn

©2013 Chinese Physical Society and the Institute of High Energy Physics of the Chinese Academy of Sciences and the Institute of Modern Physics of the Chinese Academy of Sciences and IOP Publishing Ltd

A laser diode was used to light the PMT. A pulse generator (model AFG3102) was used to drive the laser diode and its synchronizing signal after converting to NIM level served as the trigger signal of FADC. The voltages to the PMTs were supplied by the high voltages system SY1527 controlled by the DAQ computer as well as the intensity and frequency of the light source. With this coincidence, triggers caused by noise can be largely suppressed. The pulse driving laser diode is 10 ns width pulse. Its voltage was carefully tuned to get single photon and multi photons.

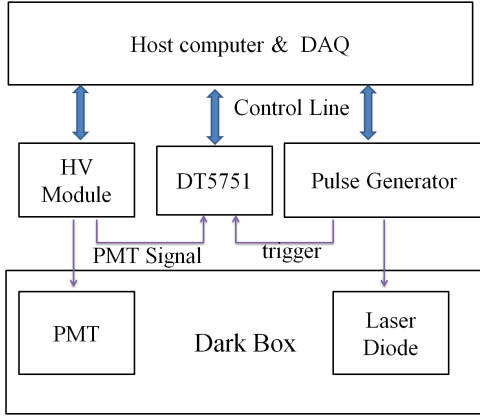


Fig. 1. The setup used for PMT performance measurements.

Another option for the test instrument was Lecroy WavePro 7100. Their technical performances and specifications were listed in Table 1[12, 13]. Since we need speed up our test procedure and demand for a large time buffer memory, DT5751 was our final choice.

Table 1. Comparison of performance parameters for DT5751 and WavePro 7100.

Instrument	DT5751	WavePro 7100
Sampling Frequency	1/(GHz/s)	10/(GHz/s)
Memory Depth	1.835/Mpts	1/Mpts
Dead time	0/ μ s	<6/ μ s
Band Width	500/MHz	1/GHz
Sensitivity	1/(mV/div)	2/(mV/div)
Weight	680/gr	18/Kg
Price	50/K	150/K

3 Results and Discussions

A detailed measurement on after pulse time and charge pattern of a 8 inch hemispherical PMT R5912[14] was tested with this measurement system. Not only the characteristic of after pulse, but also other information could be acquired by this test system, such as the signal photoelectron spectrum(SPE), TTS, dark current and so on.

3.1 Timing and Charge Distribution of after pulse

Fig. 2 shown the timing pattern of after pulses of R5912. The time of the after pulse was defined as the time interval between the main pulse and after pulse, time difference larger than 500 ns was shown in the plot. There were two groups which have distinct characteristics, representing two different types of ions. For R5912, two ion peaks were at around 1.56 μ s and 6.37 μ s, corresponding to methane and caesium ionization[15, 16]. This results were consistent with oscilloscope test results[17]. A scattered plot of after pulse charge in units of p.e. versus arrival time was also shown in Fig. 2. Most after pulses are single p.e. charge pulses, irrelevant to main pulse charge. The temporal uniformly distributed single p.e. charge hits were caused by PMT dark noise.

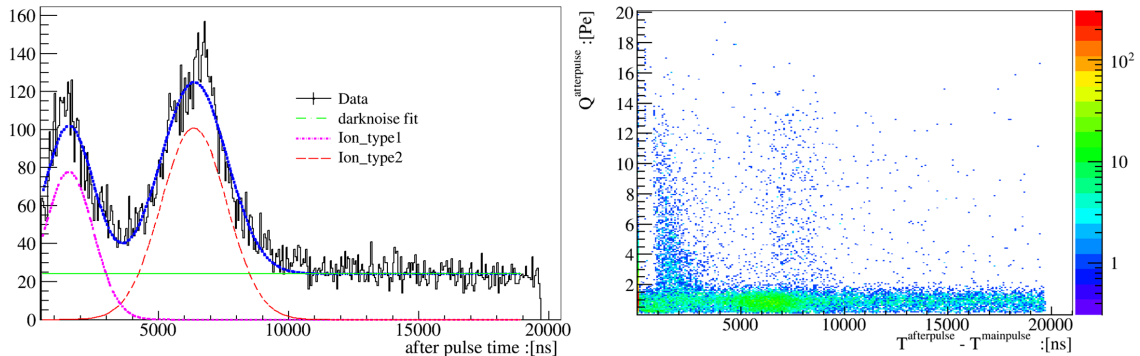


Fig. 2. (left) After pulse time distribution. (right) After pulse time(x axis) and charge (y axis in units of p.e.) distribution. The long and narrow band was dark noise.

Besides the after pulse signal reported in Ref. [15–17], we had also observed a fast component after pulse, which occurred at around 50 ns after the initial pulse, mainly single p.e. pulses. Since many PMT test sys-

tems use discriminator, this type of after pulse can be suppressed completely by the discriminator dead time (≈ 200 ns)[18]. This type of after pulses' charge and time characteristics were presented in Fig. 3.

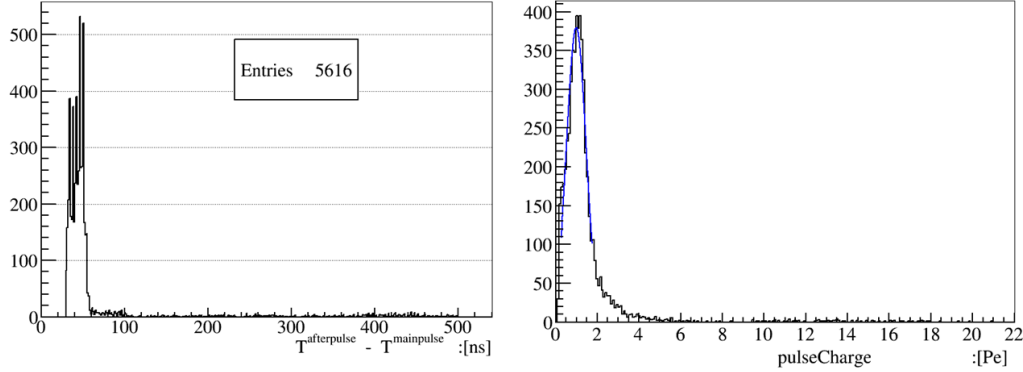


Fig. 3. (left) Fast after pulse time distribution (right) Fast after pulse charge distribution in units of p.e.

3.2 Absolute transit time and transit time spread

The fast component after pulse arises from photoelectrons hitting the first dynode backscattered. The backscattered photoelectrons were decelerated by the electric field and then accelerated again towards the first dynode[19]. Thus the resulting delay time was twice the transition time of photoelectron from the photocathode to the first dynode. As a result, absolute transition time and transition time spread can be obtained from hit time distribution of fast after pulse. The results were shown in Fig. 4 and Table 2. Using the results from high statistics after pulse, the absolute transit time for R5912 was 22.0 ns and transit time spread is 2.8 ns.

Table 2. Fitting results of hit time using three Gaussian functions.

Item	Main peak/ns	AP peak /ns	2nd AP peak/ns
Hittime	295.7	339.7	387.8
Spread	5.6	8.6	10.7

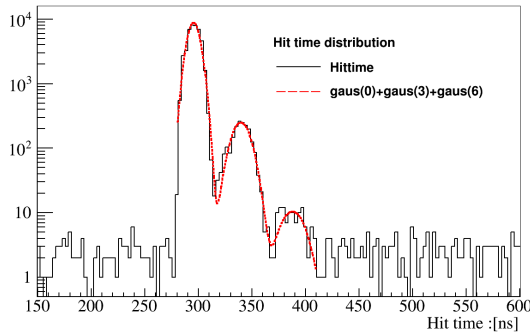


Fig. 4. Hit time of three peaks: main pulse, after pulse, after pulse caused by after pulse. The dashed line was fitting curve using three Gaussian functions.

3.3 After pulse rate and dark rate

There were various after pulse rate definitions in previous studies, such as defining the total after pulse charge and main pulse charge ratio as after pulse rate, or regarding after pulse number and main pulse charge ratio as after pulse rate[20]. Here we defined the after pulse rate as the number of after pulse seen by per p.e. of the initial pulse, same definition as in Ref. [17], after pulse rate was proportional to main pulse charge, see in Fig. 5. By this definition, we derived the after pulse rate from a one degree polynomial fit to the main pulse charge versus after pulse number plot. The offset of the linear fit function can be regarded as dark count, also illustrated in Fig. 2, which is independent of the main pulse charge. The slope of the linear fit function was after pulse rate, i.e. 1.794%. This result was in consistency with Ref. [17], 1.7%. From the offset and inspection time period, we can get PMT dark rate. In our test, the time window was 20 μ s, thus PMT dark rate at this temperature was $0.235/(20 \times 10^{-6})$, i.e. 11.75 KHz.

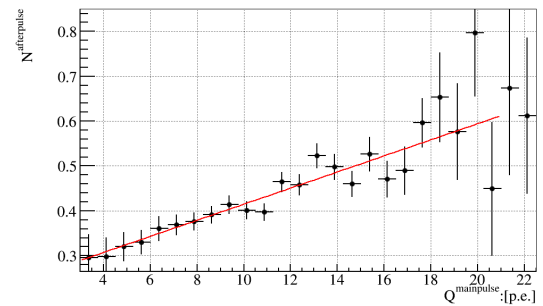


Fig. 5. After pulse number as the function of main pulse charge in p.e.

3.4 Single photoelectron spectrum and waveform

Typical single photoelectron spectrum system[21] was set up as in Ref. [21]. High precision electronics can be obtained by this system. However employing NIM crate and VME framework made the system lack of flexibility and mobility. Using the light weighted FADC system, PMTs can be tested almost anywhere and anytime. In the test procedure, we measured the single photoelectron response to calibrate the FADC. To do this, we turn our light source intensity down to ensure that SPE pulses' occupancy was less than 10% among all triggers.

Single photoelectron (SPE) study gave the distribution of the charge gain and pulse peak value. From averaged SPE waveform (Fig. 6), pulse peak and pulse rise time can also be measured, which serve as references for the PMT readout system design. To detect peaks, a scan for threshold crossing in pedestal-subtracted waveform was performed. Some algorithm was applied to extract peaks from the waveform and get charge and hit time for each peak. From the averaged single p.e. waveform, we could derive some information, such as the rising time was 4.8 ns and the SPE amplitude is 10.897 mV, etc.

A similar charge calculation algorithm bearing a resemblance to V965 QDC, produce a single photoelectron charge spectrum. From the spectrum, the common cited

Peak/valley ratio was 3.821. And PMT charge gain can be calculated from the charge spectrum by doing a double Gaussian fit to the spectrum:

$$Gain = \frac{Q^{spe} - Q^{pedestal}}{Q^{electron}}. \quad (1)$$

Here, Q^{spe} and $Q^{pedestal}$ was from double Gaussian fit, the gain by DT5751 is 6.375×10^6 , with agreement to the result from V965 6.438×10^6 , shown in Fig. 7.

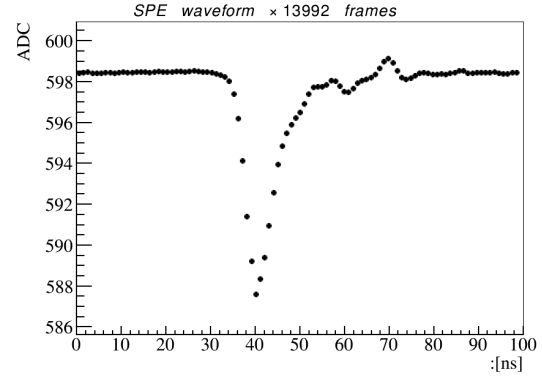


Fig. 6. Typical SPE waveform(averaged from 13882 frames).

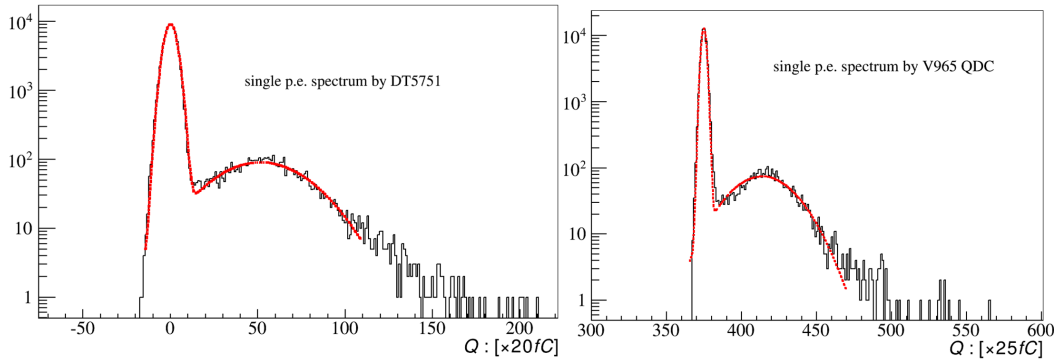


Fig. 7. (left) charge spectrum of SPE by DT5751 (right) charge Spectrum by V965 QDC.

4 Conclusion

We studied the possibility to measure after pulse with FADC and design an experiment scheme which can finalize after pulse test in almost one hour taking advantage of zero dead time of Flash ADC. Meanwhile, it took over ten hours for oscilloscope to get equivalent statistics of after pulse. We measured one 8 inch Hamamatsu PMTs' after pulse with high precision and get plenty of useful information by employing waveform analysis. These characters of every single PMT, such as gain, dark rate, pre-pulse and after pulse, absolute PMT transition time and its spread can be derived by applying this FADC test system. The system can help PMT performance study

and will play an important role in batch PMT testing for next generation reactor neutrino experiments, such as Jiangmen Underground Neutrino Observatory. Since waveform sampling is the trend for high energy physics experiment read-out system, such studies based on standalone FADC is a salutary attempt.

5 Acknowledgments

The project supported by the National Natural Science Foundation of China (Grant No. 10775181), and the Strategic Priority Research Program of the Chinese Academy of Sciences (Grant No. XDA10010200 & No. XDA10010400).

References

- 1 Y. Fukuda *et al.* [Super-Kamiokande Collaboration], Phys. Rev. Lett. **81**(8):1562 (1998)
- 2 F. P. An *et al.* [Daya Bay Collaboration], Phys. Rev. Lett. **108** 171803 (2012)
- 3 Tripathi *et al.* Nucl. Instrum. Methods A **497**(2):331. (2003)
- 4 G.A. Morton *et al.* IEEE Trans. Nucl. Sci. **14** 443 (1967)
- 5 I. Fedorko *et al.* ATL-COM-TILECAL-99-015, (1999).
- 6 Creusot *et al.* Nucl. Instrum. Methods A **725** :144. (2013)
- 7 G.A. Morton *et al.* IEEE Trans. Nucl. Sci. NS-14443 (1967).
- 8 Akchurin N *et al.* Nucl. Instrum. Methods A **574** 121 (2007)
- 9 Akgun *et al.* Nucl. Instrum. Methods A **550**(1):145-156. (2005)
- 10 cp.literature.agilent.com/litweb/pdf/5990-8780EN.pdf
- 11 <http://www.caen.it/csite/CaenProd.jsp?parent=14&idmod=632>
- 12 http://www.atecorp.com/ATECorp/media/pdfs/data-sheets/LeCroy-Wavepro7000-Series_Datasheet.pdf
- 13 www.caen.it/servlet/checkCaenManualFile?Id=9328
- 14 http://www.hamamatsu.com/resources/pdf/etd/LARGE_AREA_PMT_TPMH1286E05.pdf
- 15 Julia Haser *et al.* physics.ins-det 11 Jan (2013)
- 16 Aguil E *et al.* Nucl. Instrum. Methods A **538**(1):255-264.(2005)
- 17 S.Jetter *et al.* Chin. Phys. C **36**:733 (2012)
- 18 Funck E. Nucl. Instrum. Methods A **245**(2):519. (1986)
- 19 Kaether F *et al.* Journal of Instrumentation, 7(09):P09002. (2012)
- 20 Akgun U *et al.* Journal of Instrumentation, 3(01):T01001. (2008)
- 21 Sen Qian *et al.* Proc. of SPIE Vol. 7847, 784708-10, (2010)